

Sequential Function-Space Variational Inference via Gaussian Mixture Approximation

Menghao Waiyan William Zhu¹ Pengcheng Hao Ercan Engin Kuruoğlu
Tsinghua Shenzhen International Graduate School
Shenzhen, China

Abstract—Continual learning is learning from a sequence of tasks with the aim of learning new tasks without forgetting old tasks. Sequential function-space variational inference (SFSVI) is a continual learning method based on variational inference which uses a Gaussian variational distribution to approximate the distribution of the outputs of a finite number of selected inducing points. Since the posterior distribution of a neural network is multi-modal, a Gaussian distribution could only match one mode of the posterior distribution, and a Gaussian mixture distribution could be used to better approximate the posterior distribution. We propose an SFSVI method which uses a Gaussian mixture variational distribution. We also compare different types of variational inference methods with and without a fixed pre-trained feature extractor. We find that in terms of final average accuracy, Gaussian mixture methods perform better than Gaussian methods and likelihood-focused methods perform better than prior-focused methods.

Index Terms—Bayesian inference, class-incremental learning, continual learning, domain-incremental learning, variational inference

I. INTRODUCTION

When neural networks learn new tasks, they lose predictive performance on old tasks. This is known as catastrophic forgetting [1]. It can be prevented by training using all the data, which we refer to as joint maximum a posteriori (MAP) training. However, access to the previous data may be limited due to computational or privacy constraints, so the aim of continual learning is to prevent forgetting with little or no access to the previous data.

For classification tasks, three types of continual learning settings are commonly studied [2]:

- 1) **Task-incremental learning**, in which task IDs are provided and the classes change between tasks
- 2) **Domain-incremental learning**, in which task IDs are not provided and the classes remain the same between tasks but the input data distribution changes between tasks
- 3) **Class-incremental learning**, in which task IDs are not provided and the classes change between tasks

In task-incremental learning, a multi-headed neural network is typically used, in which there is one head per task and the task ID is used to determine the head to use for prediction. In

domain- and class-incremental learning, a single-headed neural network is typically used.

Task IDs make continual learning much easier by restricting the possible classes and are unlikely to be accessible in practice. We adhere to the desiderata proposed in [3] and focus on domain- and class-incremental learning with single-headed neural networks on task sequences with more than two similar tasks and limited access to the previous data.

Continual learning methods are commonly classified into regularization-based methods, memory- or replay-based methods and parameter-isolation-based methods [4]. The last class of method is mainly used for task-incremental learning with a multi-headed neural network. We are mainly concerned with regularization-based and replay-based methods with single-headed neural networks based on Bayesian inference.

For a single-headed neural network with fixed architecture, sequential Bayesian inference can be performed on the neural network parameters, in which the previous posterior distribution becomes the current prior distribution, and prediction is provided by the posterior predictive distribution. There is a class of method based on sequential maximum a posteriori inference (SMI) which performs a quadratic approximation of the previous posterior probability density function (PDF). We focus on another class of method called sequential variational inference (SVI).

In SVI, the posterior distribution is approximated with a simple parametric variational distribution by minimizing its Kullback-Leibler (KL) divergence from the posterior distribution. Since the goal of learning is prediction, it is reasonable to approximate the predictive distribution of the neural network output before the final activation function. This approach is known as a function-space approach, and we refer to the classical approach as a parameter-space approach.

[5] describes two general ways of performing SVI. In a prior-focused approach, the previous variational distribution is used as the current prior distribution, while in a likelihood-focused approach, the prior distribution is not updated, and the previous likelihood functions are approximated with stored or generated previous data. Thus, prior-focused approaches are mostly regularization-based, and likelihood-focused approaches are mostly replay-based.

The Gaussian distribution with a diagonal covariance matrix is the most commonly used variational distribution. However, it can only match one mode of the posterior distribution. A

Correspondence to: Menghao Waiyan William Zhu (zhumh22@mails.tsinghua.edu.cn)

Gaussian mixture variational distribution can be used to match multiple modes of the posterior distribution. Moreover, the Gaussian mixture distribution is also a well known approximation for heavy-tailed distributions such as Student’s t and alpha-stable distributions [6].

We propose a method for learning a Gaussian mixture variational distribution via a function-space approach. Our main goal is to investigate whether Gaussian mixture methods perform better than Gaussian methods. We also combine likelihood-focused and function-space approaches and compare prior-focused and likelihood-focused approaches. Finally, since a fixed pre-trained feature extractor can be used to reduce the high computational cost of function-space approaches, we also investigate the usefulness of a fixed pre-trained feature extractor for these methods.

II. BACKGROUND

We introduce sequential Bayesian inference and describe three methods of SVI, which our proposed method builds upon. We use bold letters to denote random variables, and the difference between vectors and scalars should be clear from context.

A. Sequential Bayesian Inference

We describe a probabilistic model for Bayesian continual learning. Let θ be the collection of parameters of the neural network and $(\mathbf{x}_\tau)_{\tau=1}^t$ and $(\mathbf{y}_\tau)_{\tau=1}^t$ be the inputs and outputs from time 1 to t , respectively. $(\mathbf{x}_\tau)_{\tau=1}^t$ are assumed to be independent, and $(\mathbf{y}_\tau)_{\tau=1}^t$ are assumed to be conditionally independent given θ and $(\mathbf{x}_\tau)_{\tau=1}^t$. These assumptions are depicted in Figure 1.

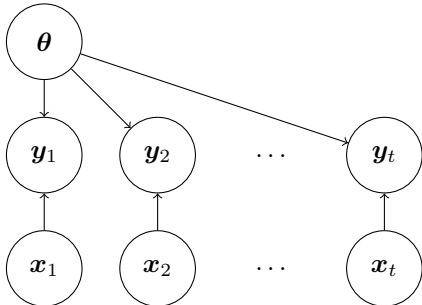


Fig. 1: Bayesian network for continual learning. θ is the collection of parameters of the neural network, $(\mathbf{x}_\tau)_{\tau=1}^t$ are the inputs and $(\mathbf{y}_\tau)_{\tau=1}^t$ are the outputs.

Note that $(\mathbf{x}_\tau, \mathbf{y}_\tau)_{\tau=1}^t$ are not necessarily identically distributed, but tasks are similar, i.e. the form of the likelihood function $l_\tau(y_\tau|\theta, x_\tau)$ is the same for all tasks. For example, in multi-class classification, it is the categorical likelihood function for all tasks. θ is assumed to be a continuous random variable of an appropriate dimension, so it has a PDF.

The posterior PDF of θ given the training data $\mathbf{D}_t = (\mathbf{x}_\tau, \mathbf{y}_\tau)_{\tau=1}^t$ is provided by Bayes’ rule:

$$p_t(\theta|\mathbf{D}_t) = \frac{1}{z_t} p_{t-1}(\theta|\mathbf{D}_{t-1}) l_t(y_t|\theta, x_t) \quad (1)$$

where $z_t = \int_{\Theta} p_{t-1}(\theta|\mathbf{D}_{t-1}) l_t(y_t|\theta, x_t) d\theta$ is a normalization constant.

The posterior predictive function of a testing output \tilde{y} given a testing input $\tilde{x} = \tilde{x}$ and the training data $\mathbf{D}_t = \mathbf{D}_t$ is the expectation of the likelihood function with respect to the posterior distribution of θ :

$$\begin{aligned} \tilde{p}_t(\tilde{y}|\tilde{x}, \mathbf{D}_t) &= \int_{\Theta} p_t(\theta|\mathbf{D}_t) l_t(\tilde{y}|\theta, \tilde{x}) d\theta \\ &= \mathbf{E}_{p_t} [l_t(\tilde{y}|\theta, \tilde{x})] \end{aligned} \quad (2)$$

B. Gaussian Variational Continual Learning

Gaussian variational continual learning (G-VCL) [7] approximates the posterior PDF of θ at time t with a Gaussian variational distribution q_t by minimizing its KL divergence from the posterior PDF of θ , which is equivalent to minimizing the variational free energy (VFE) with respect to the parameters ϕ of the variational PDF for $t = 1, 2, \dots$:

$$\mathcal{L}_t(\phi) = \mathbf{E}_{q_t} [l_t(\theta)] + D_{KL}(q_t||q_{t-1}) \quad (3)$$

where l_t is the negative log likelihood function at time t and q_0 is the prior PDF at time 1. The training method is known as Bayes by Backprop [8]. The mean vector is μ . The covariance matrix is diagonal, and its diagonal elements are given by $\sigma_i^2 = (\text{softplus}(\rho_i))^2$, where ρ_i is a real number which we refer to as the modified standard deviation. Therefore, the parameters to optimize are $\phi = (\mu, \rho)$.

To perform gradient descent on Equation (3), a ”reparameterization trick” is used to compute the expectation term in Equation (3), which is essentially rewriting the neural network parameter θ as a function of the variational parameters ϕ and a standard random variable:

$$\theta = \mu + \text{softplus}(\rho) \odot \mathbf{z} \quad (4)$$

where \odot is element-wise multiplication and \mathbf{z} is the standard Gaussian random variable with the same dimension as θ . The expectation is approximated by taking a standard sample, applying Equation (4) and computing the average l_t based on the sample. The KL divergence can be computed in closed form or approximated similarly. In mini-batch gradient descent, it is divided by the number of batches in the dataset, which is known as KL reweighting.

C. Gaussian Mixture Variational Continual Learning

Gaussian mixture variational continual learning (GM-VCL) [9] uses a Gaussian mixture variational distribution to perform parameter-space variational inference. A Gaussian mixture distribution is a categorical mixture of Gaussian distributions, i.e., there is a categorical random variable κ with k categories such that given $\kappa = \kappa$, θ is conditionally Gaussian. It has a categorical probability mass function (PMF) with probabilities $(p_i)_{i=1}^k$, and we will refer to κ as the mixing categorical random variable. Thus, the variational distribution has PDF $\sum_{\kappa=1}^k p_\kappa f_\kappa(\theta)$, where f_κ is the Gaussian PDF of the κ -th component.

In order to make Equation (3) differentiable, the categorical distribution is approximated with a Gumbel-softmax distribution [10], [11], which is a continuous probability distribution over the probability simplex in \mathbb{R}^k . The reparameterization trick for the Gumbel-softmax random variable $\tilde{\kappa}$ is

$$\tilde{\kappa} = \text{softmax}\left(\frac{1}{T}(\lambda + \mathbf{g})\right) \quad (5)$$

where T is a parameter known as the temperature, λ is a real vector of un-normalized log probabilities of the categories and \mathbf{g} is a standard Gumbel random variable in \mathbb{R}^k . $\tilde{\kappa}$ converges in distribution to κ as $T \rightarrow 0$, so a small T can be used for the approximation. Then, the reparameterization trick for θ is

$$\theta = \sum_{i=1}^k \tilde{\kappa}_i \theta_i \quad (6)$$

where $\tilde{\kappa}_i$ is the i -th component of $\tilde{\kappa}$ and θ_i is the i -th Gaussian component, i.e. θ given $\kappa = \kappa_i$.

The expectation in Equation (3) can be approximated by using the reparameterization trick in Equation (6). The KL divergence for Gaussian mixture distributions does not have a closed form expression, so it can be approximated in the same way. Alternatively, it may be replaced with an upper bound which has a closed-form expression:

$$\begin{aligned} \tilde{D}_{KL}(q_t \| q_{t-1}) &= D_{KL}(q_{t,\kappa} \| q_{t-1,\kappa}) \\ &+ \sum_{\kappa=1}^k p_{t,\kappa} D_{KL}(q_{t,\theta_\kappa} \| q_{t-1,\theta_\kappa}) \end{aligned} \quad (7)$$

where $q_{t,\kappa}$ is the variational mixing categorical PMF at time t , $p_{t,\kappa}$ is the κ -th variational mixing categorical probability at time t and q_{t,θ_κ} is the variational PDF of the κ -th Gaussian component at time t . In words, the first term is the KL divergence of the current mixing categorical PMF from the previous mixing categorical PMF, and the second term is a weighted sum of the KL divergences of the current Gaussian PDFs from the previous Gaussian PDFs, weighted by the current mixing categorical probabilities.

D. Gaussian Sequential Function-Space Variational Inference

Gaussian sequential function-space variational inference (G-SFSVI) [12] aims to directly approximate the posterior predictive distribution of $\mathbf{f}(x) = f(x; \theta)$, where f is the neural network function before the final activation function. $\mathbf{f}(x)$ can be viewed as a random process indexed by the input x , i.e. for fixed x , it is a random variable. We perform an affine approximation of f around μ :

$$\tilde{\mathbf{f}}(x; \theta) = f(x; \mu) + J_\mu(x)(\theta - \mu) \quad (8)$$

where $J_\mu(x)$ is the Jacobian matrix of $f(x; \theta)$ with respect to θ at μ . Since θ has a Gaussian variational PDF, $\tilde{\mathbf{f}}(x) = \tilde{\mathbf{f}}(x; \theta)$ is a Gaussian process indexed by x with mean function $\tilde{\mu}(x) = f(x; \mu)$ and covariance function $\tilde{\Sigma}(x_1, x_2) = J_\mu(x_1)\Sigma(J_\mu(x_2))^T$, where Σ is the diagonal covariance matrix.

Then, the VFE involves a KL divergence of Gaussian processes, which is intractable. To make it tractable, a technical assumption called "prior conditional matching" is made [13], and the KL divergence of Gaussian processes is replaced with a KL divergence of Gaussian PDFs of a finite number of inducing points:

$$\mathbf{E}_{q_t}[\mathfrak{l}_t(\theta)] + D_{KL}(\tilde{q}_t \| \tilde{q}_{t-1}) \quad (9)$$

where \tilde{q}_t is the variational PDF at time t of the inducing outputs $\tilde{\mathbf{f}}_I = (\tilde{\mathbf{f}}(x_i))_{i=1}^n$, where $(x_i)_{i=1}^n$ are the inducing inputs. The KL divergence can be computed in closed form, but in order to simplify the computation, diagonalization is made so that the covariances between different inducing points and between different output components are ignored. In particular, for all pairs of inducing points (x_1, x_2) , in the output covariance matrix $\tilde{\Sigma}(x_1, x_2) = J_\mu(x_1)\Sigma(J_\mu(x_2))^T$, all the entries are set to zero if $x_1 \neq x_2$, and all the off-diagonal entries are set to zero if $x_1 = x_2$.

III. GAUSSIAN MIXTURE SEQUENTIAL FUNCTION-SPACE VARIATIONAL INFERENCE

We propose a method which performs SFSVI with a Gaussian mixture variational PDF of θ with k components. Let κ be the mixing categorical random variable with mixing categorical probabilities $(p_i)_{i=1}^k$. We perform a conditional affine approximation of f around μ_κ given $\kappa = \kappa$, where $\kappa = 1, 2, \dots, k$:

$$\tilde{f}(x; \theta) = f(x; \mu_\kappa) + J_{\mu_\kappa}(x)(\theta - \mu_\kappa) \quad (10)$$

The following proposition states that it is a mixture of Gaussian processes.

Proposition 1. $\tilde{\mathbf{f}}(x) = \tilde{\mathbf{f}}(x; \theta)$ defined in Equation (10) is a mixture of Gaussian processes indexed by x with k components, the κ -th component having mixing probability p_κ , mean function $\tilde{\mu}_\kappa(x) = f(x; \mu_\kappa)$ and covariance function $\tilde{\Sigma}_\kappa(x_1, x_2) = J_{\mu_\kappa}(x_1)\Sigma_\kappa(J_{\mu_\kappa}(x_2))^T$.

See proof in Appendix A.

Similarly to G-SFSVI, the KL divergence of mixtures of Gaussian processes is replaced with a KL divergence of Gaussian mixture PDFs of a finite number of inducing points as in Equation (9). The KL divergence cannot be computed in closed form. It can be either computed using Monte Carlo integration or replaced with an upper bound as in GM-VCL, leading to the following VFE:

$$\begin{aligned} \mathfrak{L}_t(\phi) &= \mathbf{E}_{q_t}[\mathfrak{l}_t(\theta)] + D_{KL}(q_{t,\kappa} \| q_{t-1,\kappa}) \\ &+ \sum_{\kappa=1}^k p_{t,\kappa} D_{KL}(\tilde{q}_{t,\theta_\kappa} \| \tilde{q}_{t-1,\theta_\kappa}) \end{aligned} \quad (11)$$

where \mathfrak{l}_t is the negative log likelihood with respect to the data at time t , $q_{t,\kappa}$ is the variational mixing categorical PMF at time t , $p_{t,\kappa}$ is the κ -th variational mixing categorical probability at time t and $\tilde{q}_{t,\theta_\kappa}$ is the variational PDF of the κ -th Gaussian component at time t of the inducing outputs $\tilde{\mathbf{f}}_I = (\tilde{\mathbf{f}}(x_i))_{i=1}^n$, where $(x_i)_{i=1}^n$ are the inducing inputs. Here,

$\phi = (\lambda, (\mu_{\kappa})_{\kappa=1}^k, (\rho_{\kappa})_{\kappa=1}^k)$, where λ is the log un-normalized probabilities of the mixing categorical PMF, $(\mu)_{\kappa=1}^k$ and $(\rho)_{\kappa=1}^k$ are the means and modified standard deviations of the k Gaussian components.

By Proposition 1, the κ -th component has mixing probability p_{κ} , mean $\tilde{\mu}_{\kappa}(x) = f(x; \mu_{\kappa})$ for every inducing point x and covariance matrix $\tilde{\Sigma}_{\kappa}(x_1, x_2) = J_{\mu_{\kappa}}(x_1) \Sigma_{\kappa} (J_{\mu_{\kappa}}(x_2))^T$ for every pair of inducing points (x_1, x_2) . As in G-SFSVI, diagonalization is made so that the covariances between different inducing points and between different output components are ignored. After the diagonalization, the κ -th Gaussian component of the outputs has a mean and a variance, each of dimension nd , where n is the number of inducing points and d is the output dimension, i.e. the number of classes in classification tasks. The KL divergence of the κ -th Gaussian PDFs can be computed in closed form:

$$D_{KL}(\tilde{q}_{t, \theta_{\kappa}} \| \tilde{q}_{t-1, \theta_{\kappa}}) = \frac{1}{2} \sum_{j=1}^{nd} \left(\ln \frac{\sigma_{t-1, \kappa, j}^2}{\sigma_{t, \kappa, j}^2} - 1 \right) + \frac{1}{2} \sum_{j=1}^{nd} \frac{\sigma_{t, \kappa, j}^2 + (\mu_{t, \kappa, j} - \mu_{t-1, \kappa, j})^2}{\sigma_{t-1, \kappa, j}^2} \quad (12)$$

The KL divergence of the mixing categorical PMFs can also be computed in closed form:

$$D_{KL}(q_{t, \kappa} \| q_{t-1, \kappa}) = \sum_{\kappa=1}^k p_{t, \kappa} \ln \frac{p_{t, \kappa}}{p_{t-1, \kappa}} \quad (13)$$

The reparameterization trick for θ is as in Equation (6), where the mixing categorical distribution is approximated with a Gumbel-softmax distribution in order to make Equation (11) differentiable. When using mini-batch gradient descent to optimize the objective, the KL divergence is scaled by multiplying with the ratio of the current data batch size to the coreset batch size.

In both G-SFSVI and GM-SFSVI, a coreset, which is a small dataset of stored previous data, may be used in two ways by adopting the ideas from [5]:

- 1) **Prior-focused**: The coreset is used to sample the inducing points from the second task on. The variational posterior PDF of the current task is used as the prior PDF of the next task. This is the approach used in the original G-SFSVI [12].
- 2) **Likelihood-focused**: The coreset is used to approximate the previous likelihood functions, and the inducing points are sampled uniformly from the input space for all tasks. The prior PDF is not updated:

$$\mathbf{E}_{q_t} \left[\sum_{i=1}^t \ell_i(\theta) \right] + D_{KL}(\tilde{q}_t \| \tilde{q}_0) \quad (14)$$

IV. RELATED WORK

In Section II, we have already described three related works based on SVI, namely Gaussian variational continual learning

(G-VCL) [7], Gaussian mixture variational continual learning (GM-VCL) [9] and Gaussian sequential function-space variational inference (G-SFSVI) [12]. There are also some other works that use the function-space approach. Functional regularization of the memorable past [14] uses a Laplace approximation to approximate the output distribution. Functional regularization for continual learning [15] uses variational inference on the final layer and treats the earlier layers as deterministic parameters to be optimized.

Another approach to Bayesian continual learning is based on sequential MAP inference (SMI), typically using a quadratic approximation of the previous loss function as a regularization term, so these methods rely on approximating the Hessian matrix. Elastic weight consolidation (EWC) uses a diagonal approximation of the empirical Fisher information matrix (eFIM) [16], adding a quadratic term to the objective for every task. [17] proposes a corrected objective with a single quadratic term for which the eFIM can be cumulatively added. Synaptic intelligence (SI) uses the change in loss during optimization to give a diagonal approximation [18]. Online structured Laplace approximation uses Kronecker factorization to perform a block-diagonal approximation [19].

We build upon the methods described in Section II and perform function-space variational inference using a Gaussian mixture variational distribution. We also apply the idea of prior-focused and likelihood-focused approaches and ask whether it is better to use the coreset for the KL divergence term or the expected negative log likelihood term.

V. EXPERIMENTS

We first perform experiments on small task sequences to visualize the prediction probabilities. Then, we perform experiments on image task sequences. In each experiment, the final average accuracy of different SVI methods are compared with reference methods, SMI methods and SVI methods. Each task sequence has training, validation and testing dataset sequences. Data used, methods compared and results obtained are described below. More details can be found in Appendix B.

A. Data

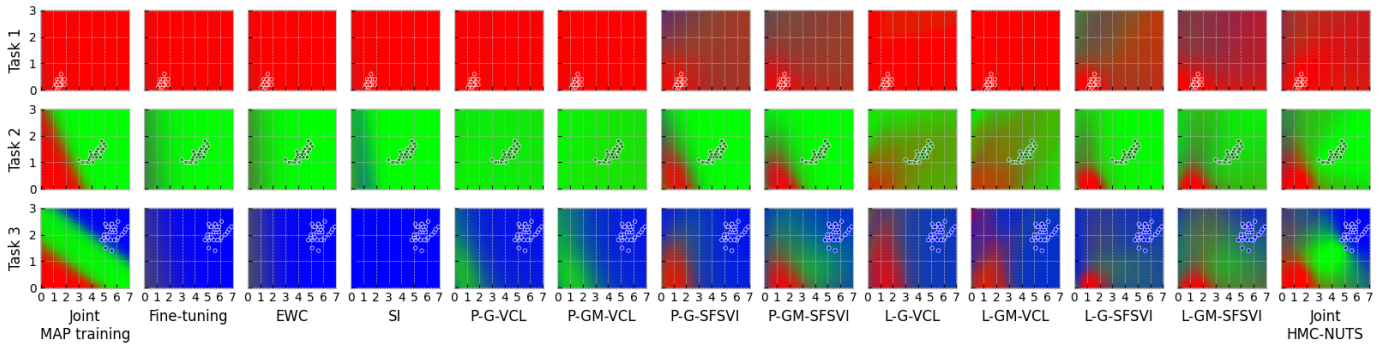
CI indicates class-incremental learning, and DI indicates domain-incremental learning.

The task sequences used for the visualizations are:

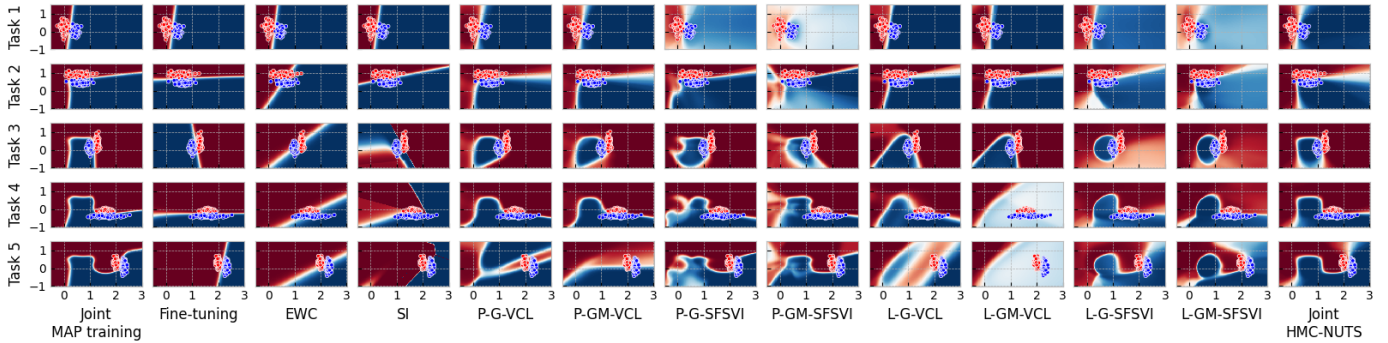
- **CI Split 2D Iris**: A task sequence for flower species classification based on Iris and consists of 3 tasks, each with 1 class.
- **DI Sinusoid**: A synthetic task sequence used in [12] and consists of 5 tasks, each with 2 classes.

The image task sequences used are:

- **CI Split MNIST** and **DI Split MNIST**: A task sequence for handwritten digit classification based on MNIST and consists of 5 tasks, each with 2 classes. In DI Split MNIST, the classes are set to even and odd. The pre-training task for them is **EMNIST Letters**, which has no classes in common with them.



(a) CI Split 2D Iris. The x-axis is the petal length (cm) and the y-axis is the petal width (cm). The pseudocolor plot shows the prediction probabilities mapped to the red, green and blue color channels, and the dots show the observed data. P-GM-SFSVI and L-GM-SFSVI could remember the second class (green) better than their Gaussian counterparts.



(b) DI Sinusoid. The x-axis and y-axis are the two axes for the synthetic data. The pseudocolor plot shows the prediction probabilities with a red-blue colormap, and the dots show the observed data. Likelihood-focused SFSVI methods show better defined class boundaries, which are more similar to those of joint HMC-NUTS, than their prior-focused counterparts.

Fig. 2: Visualizations of prediction probabilities on CI Split 2D Iris and DI Sinusoid. All Gaussian mixture methods use 3 Gaussian components. A coreset size of 16 data points per task is used for all SVI methods except P-G-VCL and P-GM-VCL.

- **CI Split CIFAR-10 and DI Split CIFAR-8:** A task sequence for natural image classification based on CIFAR-10 and consists of 5 and 4 tasks respectively, each with 2 classes. For DI Split CIFAR-8, 2 animal classes "bird" and "frog" are removed from CIFAR-10, and the classes are set to "vehicle" and "animal". The pre-training task for them is **CIFAR-100**, which has no classes in common with them.
- **CI Split HAM-8 and DI Split HAM-6:** A task sequence for skin condition classification based on HAM10000, which we rename to HAM-8 based on the number of classes, and consists of 4 and 3 tasks respectively, each with 2 classes. For domain-incremental learning, 1 benign class "vascular lesion" and 1 indeterminate class "actinic keratosis" are removed from HAM-8, and the classes are set to "benign" and "malignant". The pre-training task for them is BCN20000, which we rename to BCN-12 based on the number of classes, and has classes in common with HAM-8, but they are skin images from different populations.

B. Methods

Joint MAP training and fine-tuning serve as the best and worst reference methods, respectively. SVI method names have

3 parts indicating respectively prior-focused (P) or likelihood-focused (L), Gaussian (G) or Gaussian mixture (GM) and parameter-space (VCL) or function-space (SFSVI). We also compare with SMI methods EWC with Huszár's corrected penalty [17], [20] and SI [18]. In visualizations, we also use as a reference method joint Hamiltonian Monte Carlo - No U Turn Sampler (HMC-NUTS), which is regarded as the gold standard Bayesian method. However, since it is not scalable, it is not used in image task sequences.

SVI methods are expensive for large fully connected neural networks (FCNNs) and convolutional neural networks (CNNs). In applications where a similar task is available, we could pre-train a neural network on it and use it as a fixed pre-trained feature extractor. Then, the coreset consists of only features, and the method also becomes privacy-preserving. We perform experiments with a pre-trained feature extractor on all the aforementioned task sequences as well as without a feature extractor on CI Split MNIST and DI Split MNIST using an FCNN and a CNN and on CI Split CIFAR-10 and DI Split CIFAR-8 using a CNN. Hyperparameter tuning is done for EWC and SI, and the testing final average accuracy is evaluated for all the methods. The testing final average accuracy is the average of the accuracies on all the testing datasets of a task sequence.

TABLE I: Testing final average accuracy for the methods with and without a pre-trained feature extractor. A coreset with 256 data points per task is used for all SVI methods except P-G-VCL and P-GM-VCL. All Gaussian mixture methods use 3 Gaussian components. Gaussian mixture methods outperform Gaussian methods, and likelihood-focused methods significantly outperform prior-focused methods.

(a) With a pre-trained feature extractor

Method	CI			DI		
	Split MNIST	Split CIFAR-10	Split HAM-8	Split MNIST	Split CIFAR-8	Split HAM-6
Joint MAP training	95.1077	76.25	41.2552	93.4338	96.6250	71.0659
Fine-tuning	19.8382	19.04	22.5610	64.4789	89.6250	61.7650
EWC	73.3744	31.94	32.2972	82.9540	94.6625	68.4228
SI	30.2364	27.05	25.9327	79.4063	95.0750	68.0341
P-G-VCL	25.2223	18.96	22.8659	79.8042	92.4625	63.9840
P-GM-VCL	27.6612	19.00	23.4756	77.4632	92.8125	63.3092
P-G-SFSVI	88.7514	52.60	47.6568	91.1877	96.4000	73.8057
P-GM-SFSVI	89.2844	53.82	40.9113	91.3151	96.3000	70.8928
L-G-VCL	90.2739	64.31	53.8159	91.9639	94.6125	74.9034
L-GM-VCL	90.6559	64.68	51.6726	92.0008	94.8125	75.5949
L-G-SFSVI	91.3509	66.10	44.8271	91.6020	95.5125	76.9159
L-GM-SFSVI	92.0564	65.84	51.1982	92.1971	95.7375	77.5816

(b) Without a pre-trained feature extractor

Method	CI Split MNIST		DI Split MNIST		CI Split CIFAR-10		DI Split CIFAR-8	
	FCNN	CNN	FCNN	CNN	CNN	CNN	CNN	CNN
Joint MAP training	97.9428	99.0519	98.6771	99.4347	76.1400		95.9750	
Fine-tuning	19.8891	19.9496	54.9867	61.9545	19.2500		87.1625	
EWC	21.5787	19.9697	68.4412	72.9213	19.8300		89.2625	
SI	20.7597	20.3879	60.2053	72.4020	19.8900		89.0250	
P-G-VCL	10.1765	10.1664	59.9472	69.6936	10.0000		88.6750	
P-GM-VCL	10.1765	9.8235	56.6284	73.0150	10.0000		88.1125	
P-G-SFSVI	41.0995	29.8362	76.4496	84.9821	18.7300		88.9875	
P-GM-SFSVI	40.3262	28.8239	76.1708	91.5442	18.5500		89.3125	
L-G-VCL	43.5818	80.8643	94.2151	97.5226	20.3400		89.8000	
L-GM-VCL	44.2003	79.8097	94.7914	97.3788	10.0000		90.2875	
L-G-SFSVI	92.3369	96.9623	96.0761	98.4330	45.4800		91.4250	
L-GM-SFSVI	92.2116	97.2589	96.5303	98.5603	45.4900		91.9125	

C. Results

We are interested in which has better continual learning performance in terms of final average accuracy: prior-focused (P) or likelihood-focused (L), Gaussian (G) or Gaussian mixture (GM) and parameter-space (VCL) or function-space (SFSVI).

The visualizations of prediction probabilities for all the methods are shown in Figure 2. We find that the likelihood-focused methods give slightly more accurate prediction probabilities than prior-focused methods. The function-space methods give significantly more accurate prediction probabilities than their parameter-space counterparts, especially in later tasks. The advantage of Gaussian mixture function-space methods over their Gaussian counterparts are especially noticeable in CI Split 2D Iris.

The testing final average accuracy for all the experiments on image task sequences are shown in Table I. We find that likelihood-focused methods give much higher final average accuracy than prior-focused methods with or without a feature extractor. Although [12] reports a high final average accuracy for P-G-SFSVI with an FCNN on CI Split MNIST, we find that it is difficult to achieve such a high final average accuracy

for P-G-SFSVI, but using its likelihood-focused counterpart L-G-SFSVI makes it easier to achieve a high final average accuracy. On most of the task sequences, we find that L-GM-SFSVI achieves the highest final average accuracy.

VI. CONCLUSION

We proposed a method that performs sequential function-space variational inference using a Gaussian mixture variational distribution with two variants: prior-focused and likelihood-focused. We compared them with six other types of sequential variational inference methods on class- and domain-incremental task sequences with or without a fixed pre-trained feature extractor and showed empirically that the likelihood-focused Gaussian mixture sequential function-space variational inference achieves the best continual learning performance in terms of final average accuracy with or without a pre-trained feature extractor. We also showed empirically that in general, likelihood-focused methods perform significantly better than their prior-focused counterparts. We hope that our work revealed more insights into sequential variational inference methods. In the future, we may work on more

applications in medical image classification and document image understanding [21].

SOFTWARE AND DATA

All the datasets used in this work are either synthetic or publicly available. Iris is available from the `scikit-learn` package [22], which is released under the 3-clause BSD license. MNIST, EMNIST, CIFAR-10 and CIFAR-100 are available from the `pytorch` package [23], which is also released under the 3-clause BSD license. HAM10000 [24] is released by the Hospital Clinic in Barcelona under CC BY-NC, and BCN20000 [25] is released by ViDIR Group, Department of Dermatology, Medical University of Vienna, also under CC BY-NC.

Documented and reproducible code is available under an MIT Licence at <https://github.com/blackblitz/bcl>.

IMPACT STATEMENT

This paper presents work whose goal is to advance the field of continual learning. The ability to continually learn new knowledge without forgetting old knowledge has a great impact on society, especially in healthcare, where, for example, we would like to be able to learn new diseases without forgetting old diseases, or diagnosis and treatment is made as signs and symptoms progress over the course of time. Since continual learning methods inherently have some form of memory, it is important that they are designed to preserve the privacy of people.

ACKNOWLEDGEMENTS

We thank Professor Yang Li from Tsinghua Shenzhen International Graduate School and anonymous reviewers for their feedback.

REFERENCES

- [1] M. McCloskey and N. J. Cohen, “Catastrophic interference in connectionist networks: The sequential learning problem,” *Psychology of Learning and Motivation - Advances in Research and Theory*, vol. 24, C 1989.
- [2] G. M. van de Ven, T. Tuytelaars, and A. S. Tolias, “Three types of incremental learning,” *Nature Machine Intelligence*, vol. 4, no. 12, pp. 1185–1197, 2022.
- [3] S. Farquhar and Y. Gal, *Towards robust evaluations of continual learning*, 2019. arXiv: 1805.09733.
- [4] Z. Mai, R. Li, J. Jeong, D. Quispe, H. Kim, and S. Sanner, “Online continual learning in image classification: An empirical survey,” *Neurocomputing*, vol. 469, pp. 28–51, 2022.
- [5] S. Farquhar and Y. Gal, *A unifying Bayesian view of continual learning*, 2019. arXiv: 1902.06494.
- [6] E. Kuruoglu, C. Molina, S. Godsill, and W. Fitzgerald, “A new analytic representation for the symmetric α -stable probability density function,” in *Proceedings of the 5th World Meeting of the International Society for Bayesian Analysis (ISBA)*. ASA: American Statistical Association, 1997, pp. 229–233.

- [7] C. V. Nguyen, Y. Li, T. D. Bui, and R. E. Turner, “Variational continual learning,” in *International Conference on Learning Representations*, 2018.
- [8] C. Blundell, J. Cornebise, K. Kavukcuoglu, and D. Wierstra, “Weight uncertainty in neural network,” in *Proceedings of the 32nd International Conference on Machine Learning*, F. Bach and D. Blei, Eds., ser. Proceedings of Machine Learning Research, vol. 37, Lille, France: PMLR, 2015, pp. 1613–1622.
- [9] H. Phan, A. P. Tuan, S. Nguyen, N. V. Linh, and K. Than, “Reducing catastrophic forgetting in neural networks via Gaussian mixture approximation,” in *Advances in Knowledge Discovery and Data Mining*, J. Gama, T. Li, Y. Yu, E. Chen, Y. Zheng, and F. Teng, Eds., Cham: Springer International Publishing, 2022, pp. 106–117.
- [10] E. Jang, S. Gu, and B. Poole, “Categorical reparameterization with gumbel-softmax,” in *International Conference on Learning Representations*, 2017.
- [11] C. J. Maddison, A. Mnih, and Y. W. Teh, “The concrete distribution: A continuous relaxation of discrete random variables,” in *International Conference on Learning Representations*, 2017.
- [12] T. G. J. Rudner, F. B. Smith, Q. Feng, Y. W. Teh, and Y. Gal, “Continual learning via sequential function-space variational inference,” in *Proceedings of the 39th International Conference on Machine Learning*, K. Chaudhuri, S. Jegelka, L. Song, C. Szepesvari, G. Niu, and S. Sabato, Eds., ser. Proceedings of Machine Learning Research, vol. 162, PMLR, 2022, pp. 18 871–18 887.
- [13] T. G. J. Rudner, Z. Chen, and Y. Gal, “Rethinking function-space variational inference in Bayesian neural networks,” in *Third Symposium on Advances in Approximate Bayesian Inference*, 2021.
- [14] P. Pan, S. Swaroop, A. Immer, R. Eschenhagen, R. Turner, and M. E. E. Khan, “Continual deep learning by functional regularisation of memorable past,” in *Advances in Neural Information Processing Systems*, H. Larochelle, M. Ranzato, R. Hadsell, M. F. Balcan, and H. Lin, Eds., vol. 33, Curran Associates, Inc., 2020, pp. 4453–4464.
- [15] M. K. Titsias, J. Schwarz, A. G. d. G. Matthews, R. Pascanu, and Y. W. Teh, “Functional regularisation for continual learning with Gaussian processes,” in *International Conference on Learning Representations*, 2020.
- [16] J. Kirkpatrick, R. Pascanu, N. Rabinowitz, J. Veness, G. Desjardins, A. A. Rusu, K. Milan, J. Quan, T. Ramalho, A. Grabska-Barwinska, D. Hassabis, C. Clopath, D. Kumaran, and R. Hadsell, “Overcoming catastrophic forgetting in neural networks,” *Proceedings of the National Academy of Sciences of the United States of America*, vol. 114, no. 13, pp. 3521–3526, 2017.
- [17] F. Huszár, “Note on the quadratic penalties in elastic weight consolidation,” *Proceedings of the National*

Academy of Sciences of the United States of America, vol. 115, no. 11, E2496–E2497, 2018.

- [18] F. Zenke, B. Poole, and S. Ganguli, “Continual learning through synaptic intelligence,” in *Proceedings of the 34th International Conference on Machine Learning*, D. Precup and Y. W. Teh, Eds., ser. Proceedings of Machine Learning Research, vol. 70, PMLR, 2017, pp. 3987–3995.
- [19] H. Ritter, A. Botev, and D. Barber, “Online structured Laplace approximations for overcoming catastrophic forgetting,” in *Advances in Neural Information Processing Systems*, S. Bengio, H. Wallach, H. Larochelle, K. Grauman, N. Cesa-Bianchi, and R. Garnett, Eds., vol. 31, Curran Associates, Inc., 2018.
- [20] F. Huszár, *On quadratic penalties in elastic weight consolidation*, 2017. arXiv: 1712.03847.
- [21] E. E. Kuruoğlu and A. S. Taylor, “Using annotations for summarizing a document image and itemizing the summary based on similar annotations,” US7712028B2, 2010.
- [22] F. Pedregosa, G. Varoquaux, A. Gramfort, V. Michel, B. Thirion, O. Grisel, M. Blondel, P. Prettenhofer, R. Weiss, V. Dubourg, J. Vanderplas, A. Passos, D. Cournapeau, M. Brucher, M. Perrot, and E. Duchesnay, “Scikit-learn: Machine learning in Python,” *Journal of Machine Learning Research*, vol. 12, pp. 2825–2830, 2011.
- [23] J. Ansel, E. Yang, H. He, N. Gimelshein, A. Jain, M. Voznesensky, B. Bao, P. Bell, D. Berard, E. Burovski, G. Chauhan, A. Chourdia, W. Constable, A. Desmaison, Z. DeVito, E. Ellison, W. Feng, J. Gong, M. Gschwind, B. Hirsh, S. Huang, K. Kalambarkar, L. Kirsch, M. Lazos, M. Lezcano, Y. Liang, J. Liang, Y. Lu, C. Luk, B. Maher, Y. Pan, C. Puhersch, M. Reso, M. Saroufim, M. Y. Siraichi, H. Suk, M. Suo, P. Tillet, E. Wang, X. Wang, W. Wen, S. Zhang, X. Zhao, K. Zhou, R. Zou, A. Mathews, G. Chanan, P. Wu, and S. Chintala, “PyTorch 2: Faster Machine Learning Through Dynamic Python Bytecode Transformation and Graph Compilation,” in *29th ACM International Conference on Architectural Support for Programming Languages and Operating Systems, Volume 2 (ASPLOS '24)*, ACM, 2024.
- [24] P. Tschandl, C. Rosendahl, and H. Kittler, “The HAM10000 dataset, a large collection of multi-source dermatoscopic images of common pigmented skin lesions,” *Scientific Data*, vol. 5, no. 1, pp. 1–9, 2018.
- [25] C. Hernández-Pérez, M. Combalia, S. Podlipnik, N. C. Codella, V. Rotemberg, A. C. Halpern, O. Reiter, C. Carrera, A. Barreiro, B. Helba, *et al.*, “BCN20000: Dermoscopic lesions in the wild,” *Scientific Data*, vol. 11, no. 1, p. 641, 2024.

We first introduce a lemma.

Lemma 1. *Let θ be an \mathbb{R}^n -valued Gaussian mixture random variable with k components, the κ -th component having mixing probability p_κ , mean vector μ_κ and covariance matrix Σ_κ . Let $\boldsymbol{\kappa}$ be the mixing categorical random variable. Consider a conditional affine transformation $T_\kappa : \mathbb{R}^n \rightarrow \mathbb{R}^d$ such that given $\boldsymbol{\kappa} = \kappa$, $T_\kappa(\theta) = A_\kappa\theta + b_\kappa$, where A_κ is a $d \times n$ real matrix and b_κ is a vector in \mathbb{R}^d . Then, $T_\kappa(\theta)$ is an \mathbb{R}^d -valued Gaussian mixture random variable with k Gaussian components, the κ -th component having mixing probability p_κ , mean vector $A_\kappa\mu_\kappa + b_\kappa$, covariance matrix $A_\kappa\Sigma_\kappa A_\kappa^T$.*

Proof. The characteristic function of θ is

$$\begin{aligned}\phi_\theta(t) &= \mathbf{E} \left[e^{it^T\theta} \right] \\ &= \mathbf{E} \left[\mathbf{E} \left[e^{it^T\theta} \mid \boldsymbol{\kappa} \right] \right] \\ &= \sum_{\kappa=1}^k p_\kappa e^{it^T\mu_\kappa - \frac{1}{2}t^T\Sigma_\kappa t}\end{aligned}$$

The second equality follows from the law of iterated expectations. The third equality follows from the definition of expectation and the characteristic function of a Gaussian random variable.

The characteristic function of $T_\kappa(\theta)$ is

$$\begin{aligned}\phi_{T_\kappa(\theta)}(t) &= \mathbf{E} \left[e^{it^T(T_\kappa(\theta))} \right] \\ &= \mathbf{E} \left[\mathbf{E} \left[e^{it^T(T_\kappa(\theta))} \mid \boldsymbol{\kappa} \right] \right] \\ &= \mathbf{E} \left[\mathbf{E} \left[e^{it^T(A_\kappa\theta + b_\kappa)} \mid \boldsymbol{\kappa} \right] \right] \\ &= \sum_{\kappa=1}^k p_\kappa e^{it^T(A_\kappa\mu_\kappa + b_\kappa) - \frac{1}{2}t^T A_\kappa\Sigma_\kappa A_\kappa^T t}\end{aligned}$$

The second equality follows from the law of iterated expectations. The third equality follows from the definition of T_κ . The fourth equality follows from the definition of the expectation and the characteristic function of an affine transformation of a Gaussian random variable.

Comparing with ϕ_θ , it is clear that $\phi_{T_\kappa(\theta)}$ is the characteristic function of a Gaussian mixture random variable with the required parameters. Therefore, $T_\kappa(\theta)$ is a Gaussian mixture random variable with the required parameters. \square

Now, we are ready to prove Proposition 1.

Proof. Given $\boldsymbol{\kappa} = \kappa$, $\tilde{f}(x; \theta)$ can be rewritten as $J_{\mu_\kappa}(x)\theta + f(x; \mu_\kappa) - J_{\mu_\kappa}(x)\mu_\kappa$, so $\tilde{f}(x; \theta)$ is a conditional affine transformation T_κ of θ such that given $\boldsymbol{\kappa} = \kappa$, $T_\kappa(\theta) = A_\kappa\theta + b_\kappa$, where $A_\kappa = J_\kappa(x)$ and $b_\kappa = f(x; \mu_\kappa) - J_{\mu_\kappa}(x)\mu_\kappa$. By Lemma 1, it is a mixture of Gaussian processes with the required parameters. \square

A. Data Preparation

For DI Sinusoid, which has 5 tasks, each with 2 classes, training, validation and testing dataset sequences are prepared by generating 100 points from a bivariate Gaussian distribution with a diagonal covariance matrix for each class and task. For CI Split 2D Iris, Iris with two features "petal length" and "petal width" is split into training and testing datasets with 20% testing size, and then the training dataset into training and validation datasets with 20% validation size, so the training, validation and testing proportions are 64%, 16% and 20%, respectively. Finally, each dataset is split by class into a dataset sequence.

For EMNIST Letters, CIFAR-100 and task sequences based on MNIST and CIFAR-10, training and testing datasets are available from PyTorch, so the training dataset is split into training and validation datasets with 20% validation size. Each dataset is then split by class into a dataset sequence.

For BCN-12 and HAM-8, the 640×450 images are resized to 32×32 with Lanczos interpolation. For all image data, the pixel values are divided by 255 so that they take values between 0 and 1. Data augmentation (e.g. flipping and cropping) is not performed.

B. Neural Network Architectures

The fully connected neural network used for DI Sinusoid and CI Split 2D Iris has 2 hidden layers each of 16 nodes. All the hidden nodes use swish activation.

The pre-trained neural network for both CI Split MNIST and DI Split MNIST has 2 convolutional layers and 2 dense layers, totaling 4 layers. Each convolutional layer has $32 \ 3 \times 3$ filters and is followed by group normalization with 32 groups, swish activation and average pooling with a size of 2×2 . The hidden dense layer has 64 nodes with swish activation. Thus, the feature dimension is 64.

The pre-trained neural network for CI Split CIFAR-10, CI Split HAM-8 DI Split CIFAR-8 and DI Split HAM-6 has 17 convolutional layers and 1 dense layer, totaling 18 layers. Each convolutional layer is followed by group normalization with 32 groups and swish activation. The 2nd to the 17th convolutional layers are arranged into 8 residual blocks, each with 2 convolutional layers, and every 2 residual blocks are followed by average pooling with a size of 2×2 . The numbers of filters for the 17 convolutional layers are 32, 64, 64, 64, 64, 128, 128, 128, 128, 256, 256, 256, 256, 512, 512, 512 and 512, respectively, and the filter sizes are all 3×3 . Thus, the feature dimension is 512.

For experiments on CI Split MNIST without a fixed pre-trained feature extractor, the FCNN consists of 2 hidden layers each of 256 nodes, and the CNN is the same as in the pre-trained neural network except that the hidden dense layer has 32 nodes instead of 64 nodes. All the hidden nodes use swish activation. For experiments on CI Split CIFAR-10 and DI Split CIFAR-8, the CNN is as before but has 4 convolutional layers

and 2 dense layers, totaling 6 layers. The number of filters for the 4 convolutional layers are 32, 32, 64 and 64, respectively. The hidden dense layer has 64 nodes.

C. Training

In all experiments, the prior PDF at time 1 is a standard Gaussian PDF (of an appropriate dimension), and an Adam optimizer is used with a one-cycle learning rate schedule.

For MAP training, the parameters are initialized by using the Lecun normal initializer for the weights and setting to zeros for the biases. For variational inference training, the parameters are initialized in the same way for the mean μ , but for the modified standard deviation ρ , they are initialized from a Gaussian distribution with mean -2 and standard deviation 0.05.

For pre-training tasks and class-incremental task sequences, each task is of multi-class classification, so categorical cross entropy is used, while for domain-incremental task sequences, each task is binary classification, so binary or Bernoulli cross entropy is used. BCN-12 is a task with severe class imbalance, so for pre-training on BCN-12, instead of the standard cross entropy, a weighted cross entropy $-\sum_{i=1}^k \frac{m}{n_i} p_i \ln q_i$ is used, where p_i is the true label indicator and q_i is the predicted probability, n_i is the frequency of the i -th class and $m = \min\{n_1, n_2, \dots, n_k\}$.

For DI Sinusoid and CI Split 2D Iris, training for each task is performed for 100 epochs with a batch size of 16 except in likelihood-focused methods, where a batch of size 16 is formed by concatenating a batch of size 8 from the current data and a batch of size 8 from the coreset. The base learning rate is 0.1 except in SFSVI methods, where it is 0.01.

Fixed pre-trained feature extractors are trained as follows. For CI Split MNIST and DI Split MNIST, pre-training is performed for 20 epochs with a base learning rate of 0.01 and a batch size of 64, and training for each task is performed similarly except SFSVI methods which use a base learning rate of 0.001. For CI Split CIFAR-10 and DI Split CIFAR-8, pre-training is performed for 20 epochs with a base learning rate of 0.001 and a batch size of 64, and training for each task is performed similarly but with a base learning rate of 0.01 for non-SFSVI methods. For CI Split HAM-8 and DI Split HAM-6, pre-training is performed for 20 epochs with a base learning rate of 0.001 and a batch size of 64, and training for each task is performed similarly but with a base learning rate of 0.01 for non-SFSVI methods.

For CI Split MNIST and DI Split MNIST without a fixed pre-trained feature extractor, the FCNN is trained for 20 epochs with a batch size of 64, except in likelihood-focused methods, where a current data batch of size 32 and a coreset batch of size 32 are concatenated. The base learning rate is 0.01 except in SFSVI methods, where it is 0.001. The CNN is trained similarly, but since it takes much more memory to train a CNN with SFSVI methods, only half the batch size is used, i.e. a batch size of 32, and for likelihood-focused methods, a current data batch size of 16 and a coreset batch size of 16.

For SFSVI methods on DI Sinusoid and CI Split 2D Iris, the inducing points are randomly generated from a uniform distribution in a hyperrectangle the boundaries of which are determined by the minimum and maximum values of the training input data across all tasks in the task sequence. For image task sequences with pre-training, the boundaries for each feature component are set to -1 and 6. For image task sequences without pre-training, the boundaries for each image pixels are set to 0 and 1. For the Gaussian mixture methods, the temperature T for the Gumbel-softmax distribution is set to 0.001.

The joint HMC-NUTS used in visualization experiments is run by using all the current and previous data for the log unnormalized posterior PDF and running 64 chains on 64 CPU cores, as opposed to the other methods which are run on a GPU. The inverse mass matrix and step size are determined by using a warmup algorithm called window adaptation, which is provided by BlackJAX, and the chains are run for 100 steps after the warmup phase. Only the final sample of size 64 is taken as the posterior sample.

D. Hyperparameter Tuning

In EWC and SI, there is a hyperparameter λ that determines the regularization strength. SI has an extra damping hyperparameter ξ . Hyperparameter tuning is performed based on the validation final average accuracy via grid search among the following values:

- EWC: $\lambda \in \{1, 10, 100, 1000, 10000\}$
- SI: $\lambda \in \{1, 10, 100, 1000, 10000\}, \xi \in \{0.1, 1.0, 10\}$